HHS Public Access

Author manuscript

Cell Rep. Author manuscript; available in PMC 2018 July 18.

Published in final edited form as:

Cell Rep. 2018 May 08; 23(6): 1754–1766. doi:10.1016/j.celrep.2018.04.032.

ATF4 Regulates CD4+ T Cell Immune Responses through Metabolic Reprogramming

Xi Yang[1,3,15], **Rui Xia**[1,6,13,15], **Cuihua Yue**[1,4,15], **Wensi Zhai**[1,4], **Wenwen Du**[1,14], **Qianting Yang**[1,5], **Huiling Cao**[10], **Xiaojuan Chen**[1,12], **Danielle Obando**[1], **Yibei Zhu**[1,6], **Xinchun Chen**[5], **Jane-Jane Chen**[11], **Jon Piganelli**[7], **Peter Wipf**[8], **Yu Jiang**[9], **Guozhi Xiao**[10], **Changping Wu**[4], **Jingting Jiang**[4], and **Binfeng Lu**[1,2,16,*]

[1]Department of Immunology, School of Medicine, University of Pittsburgh, EBST E1047, 200 Lothrop Street, Pittsburgh, PA 15261, USA

[2]University of Pittsburgh Cancer Institute, Pittsburgh, PA, USA

[3]School of Medicine, Tsinghua University, HaiDian, Beijing 100084, China

[4]Department of Oncology, the Third Affiliated Hospital, Soochow University, Changzhou 213003, Jiangsu, China

[5]Guangdong Key Laboratory for Emerging Infectious Disease, Shenzhen Key Laboratory of Infection and Immunity, Third People's Hospital, Guangdong Medical College, Shenzhen, Guangdong 518112, China

[6]Department of Immunology, Institute of Medical Biotechnology, Soochow University, Suzhou 215007, China

[7]Division of Immunogenetics, Department of Pediatrics, Rangos Research Center, Children's Hospital of Pittsburgh of UPMC, Pittsburgh, PA, USA

[8]Department of Chemistry and Department of Bioengineering, University of Pittsburgh, Pittsburgh, PA 15260, USA

[9]Department of Pharmacology and Chemical Biology, University of Pittsburgh School of Medicine, Pittsburgh, PA 15261, USA

*Correspondence: binfeng@pitt.edu.
[15]These authors contributed equally
[16]Lead Contact

SUPPLEMENTAL INFORMATION

Supplemental Information includes seven figures and four tables and can be found with this article online at https://doi.org/10.1016/j.celrep.2018.04.032.

AUTHOR CONTRIBUTIONS

X.Y. designed experiments, performed experiments, analyzed data, prepared figures, and wrote the manuscript. R.X., C.Y., W.Z., W.D., and Q.Y. performed experiments, analyzed data, and prepared figures. H.C., Xiaojuan Chen, D.O., Y.Z., and J.Y. performed experiments and analyzed data. Xinchun Chen, G.X., C.W., and J.J. provided key reagents and analyzed data. J.-J.C., J.P., and P.W. provided key reagents. B.L. designed experiments, prepared figures, and wrote the manuscript.

DECLARATION OF INTERESTS

The authors declare no competing interests.

[10]Department of Biology and Shenzhen Key Laboratory of Cell Microenvironment, South University of Science and Technology of China, Shenzhen 518055, China

[11]Institute for Medical Engineering and Science, Massachusetts Institute of Technology, Cambridge, MA, USA

[12]Department of Gastroenterology, The First Affiliated Hospital of Soochow University, Suzhou 215006, China

[13]The Second Affiliated Hospital of Soochow University, Suzhou, Jiangsu 215004, China

[14]Department of Respiratory Medicine, The First Affiliated Hospital of Soochow University, Suzhou 215006, China

SUMMARY

T cells are strongly regulated by oxidizing environments and amino acid restriction. How T cells reprogram metabolism to adapt to these extracellular stress situations is not well understood. Here, we show that oxidizing environments and amino acid starvation induce ATF4 in $CD4^+$ T cells. We also demonstrate that *Atf4*-deficient $CD4^+$ T cells have defects in redox homeostasis, proliferation, differentiation, and cytokine production. We further reveal that ATF4 regulates a coordinated gene network that drives amino acid intake, mTORC1 activation, protein translation, and an anabolic program for *de novo* synthesis of amino acids and glutathione. ATF4 also promotes catabolic glycolysis and glutaminolysis and oxidative phosphorylation and thereby provides precursors and energy for anabolic pathways. ATF4-deficient mice mount reduced Th1 but elevated Th17 immune responses and develop more severe experimental allergic encephalomyelitis (EAE). Our study demonstrates that ATF4 is critical for $CD4^+$ T cell-mediated immune responses through driving metabolic adaptation.

Graphical abstract

In Brief Oxidizing environments and availability of extracellular amino acids are major mechanisms that regulate T cell proliferation and function. Yang et al. demonstrate that ATF4 drives metabolic reprogramming, which allows $CD4^+$ T cells to adapt to these stresses.

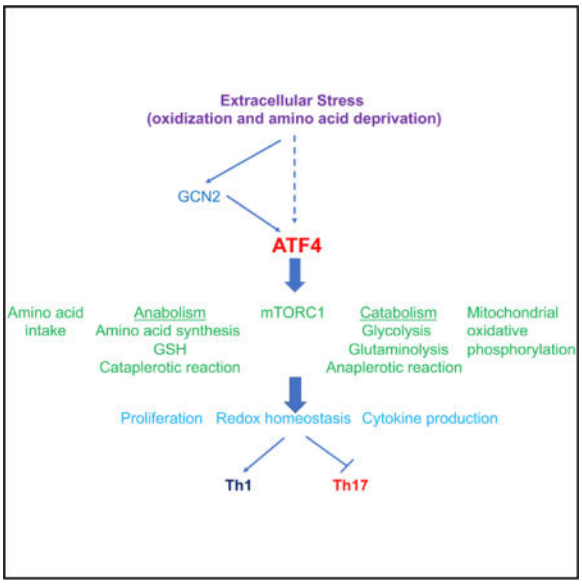

INTRODUCTION

T cell activation, proliferation, and differentiation demand striking metabolic reprogramming, which is heavily regulated by their extracellular microenvironment, particularly the oxidizing condition and availability of amino acids. There are two main mechanisms by which the extracellular oxidative environment causes stresses in T cells. First, it regulates T cell function and differentiation through oxidation of cell surface thiol groups (Kesarwani et al., 2014). This is because the surface free thiol groups are important for the function of T cells (Kesarwani et al., 2014; Pedersen-Lane et al., 2007; Sahaf et al., 2003). Second, the oxidative environment can influence T cell redox homeostasis through oxidizing extracellular cysteine and thereby restricting its availability to T cells. Cysteine is a critical precursor amino acid for the synthesis of glutathione (GSH), a major cytosolic redox buffer system (Dringen et al., 2000). During T cell activation and proliferation, GSH is important for maintaining the intracellular redox homeostasis as large amounts of reactive oxygen species (ROS) are produced by both NADPH oxidases (NOX) and mitochondria (Sena et al., 2013; Tse et al., 2010). Upon activation, T cells also accumulate biomass and at the same time secrete large amounts of cytokines. This foreseeably results in net loss of amino acids, triggering the demand for amino acids, either by *de novo* synthesis or import from the extracellular environment (Maciolek et al., 2014). As such, T cell redox homeostasis, clonal expansion, and effector functions are tightly regulated by immune suppressor cells through producing ROS and controlling the availability of amino acids. It has been proposed that myeloid-derived suppressor cells (MDSCs) inhibit T cell activation by limiting the availability of cysteine (Angelini et al., 2002; Srivastava et al., 2010). In addition, immune-suppressive myeloid cells impede T cell immune responses by restricting the availability of arginine and tryptophan (Bronte et al., 2003; Munn and Mellor, 2013). The molecular and metabolic programs underlying T cell responses to oxidative stress and amino acid deprivation are incompletely understood.

ATF4, also known as CREB2 (cAMP-response element-binding protein 2) (Karpinski et al., 1992), is a basic leucine-zipper transcription factor that is a member of the ATF/CREB protein family (Brindle and Montminy, 1992; Hai et al., 1989). *Atf4* mRNA is ubiquitously expressed throughout the body, and its protein is induced in response to various stress signals, particularly oxidative stress and amino acid deprivation, as well as endoplasmic reticulum stress (Ameri and Harris, 2008; Gjymishka et al., 2009). The stress-induced expression of ATF4 causes adaptive responses in cells through regulating the expression of target genes involved in amino acid metabolism and redox chemistry (Harding et al., 2003). ATF4 can be induced in T cells in various conditions (Harding et al., 2003; Munn et al., 2005; Sundrud et al., 2009), but the role of ATF4 in T cell metabolism and T cell-mediated immune responses is not defined.

In this study, we found the oxidizing environment and amino acid deprivation induced ATF4 in $CD4^+$ T cells. We then set out to determine how ATF4 regulates metabolic reprogramming of $CD4^+$ T cells to these stresses. In addition, we determined the role of ATF4 in $CD4^+$ T cell-mediated immune responses. The study provides mechanistic insights into T cell metabolic reprogramming in response to the extracellular oxidation and amino acid restriction.

RESULTS

Thiol Oxidation and Amino Acid Deprivation Induced ATF4 Expression in $CD4^+$ T Cells

Because of the oxidizing nature of the extracellular environment *in vitro*, cysteine is present mostly in the oxidized form, cystine (Ishii et al., 1987). It is thought that cysteine can be imported and used by T cells through its transporters ASCT1 and ASCT2 (Srivastava et al., 2010). In contrast, cystine cannot be used, because of a lack of expression of its transporter XC-in T cells (Srivastava et al., 2010). One major effect of addition of β-mercaptoethanol (β-ME), a thiol-reducing antioxidant, to the cell culture media is conversion of cystine to cysteine (Ishii et al., 1987). Addition of β-ME to a cell culture promoted T cell blasting and proliferation (Figure 1A). A gene expression study showed that a majority of top-ranked upregulated genes in T cells cultured without β-ME were ATF4 target genes (Table S1; Figure S1) (Harding et al., 2003). These data suggest that ATF4 might play an important role in adapting T cells to the thiol-oxidizing environment. Because ATF4 deficiency on the C57BL/6 genetic background resulted in embryonic lethality, we performed fetal liver transfer (FLT) experiments by infusing wild-type (WT) or $Atf4^{-/-}$ 13.5 day fetal liver cells to lethally irradiated B6 mice. We found no evidence that ATF4 affected T cell development (Figure S2). We found that both the glycine transporter 1 (*Glyt1*) and asparagine synthase (*Asns*) were upregulated in the absence of β-ME in WT but not $Atf4^{-/-}$ T cells isolated from FLT recipient mice (Figures 1B, S1A, and S1B). Similarly, addition to the culture media with acetylcysteine (NAC), a prodrug for cysteine, inhibited induction of *Asns* and *Glyt1* in an *Atf4*-dependent fashion (Figure S1A). In addition, we found that ATF4 protein was induced in activated T cells but absent in naive $CD4^+$ T cells (Figures 1C and Figure S1C). *Atf4* mRNA was abundant in naive $CD4^+$ T cells and was further elevated in cultures without β-ME (Figure S1D), indicating that *Atf4* is regulated at both transcriptional and post-transcriptional levels in T cells by extracellular oxidizing conditions. Consistent with

the requirement for *de novo* protein synthesis, the induction of *Asns* mRNA can be inhibited by rapamycin, an inhibitor for mTORC1, and cyclohexamide, an inhibitor of protein translation (Figure S3A).

Because oxidative environment reduces cysteine levels, we set out to determine whether cysteine is required for the induction of ATF4 and whether it mediates all the effect of extracellular oxidation. Our data indeed showed that *Asns* was induced by the lack of cysteine in the media (Figure 1D). Cysteine is a unique amino acid because it is both a nutrient amino acid and an antioxidant. Restricted supply of amino acids results in an increase in uncharged tRNA that binds to and activates the general control nonderepressible protein 2 (GCN2) kinase, ultimately leading to increased translation of ATF4 protein (Dong et al., 2000; Qiu et al., 2001; Vazquez de Aldana et al., 1994; Wek et al., 1989, 1995; Zhu et al., 1996). The induction of *Asns* was only partially reduced in *Gcn2*$^{-/-}$ T cells (Figure 1D). Addition of cysteine resulted in further suppression of *Asns* mRNA in both WT and *Gcn2*$^{-/-}$ T cells (Figure 1D). These results suggest that ATF4 induction by cysteine deprivation is triggered by both GCN2-dependent as well as GCN2-independent pathways (Figure 1E). Interestingly, GCN2 was not essential for ATF4 induction by the lack of β-ME in the complete media (Figure 1D). These data suggest that oxidative environment can induce ATF4 through cysteine-independent means, likely through oxidizing the cell surface thiol group (Kesarwani et al., 2014). In contrast, removal of either glutamine or leucine, the two major sources of amino acids essential for T cells (data not shown), resulted in a large induction of *Asns* mRNA levels, which was absolutely dependent on GCN2 (Figure 1D).

Besides GCN2, ATF4 protein is regulated at the translational level by double-stranded RNA-activated protein kinase (PKR), double-stranded RNA-activated protein kinase-like ER kinase (PERK), and heme-regulated inhibitor kinase (HRI). We found that PKR or HRI was not involved, but PERK was modestly involved in the induction of ATF4 in the absence of thiol-reducing antioxidant (Figures S3B–S3D). Nrf2 is a transcription factor known to be induced by oxidative stress (Zhang and Xiang, 2016). However, Nrf2 deficiency did not reduce but increased the expression of the ATF4 target gene ASNS (Figures S3B–S3D). Upon re-analysis of published expression profiling data, we found that ATF4 target genes are much higher in *Hif-1*a$^{-/-}$ CD4^{+} T cells compared with WT CD4^{+} T cells (data not shown; Shi et al., 2011). Collectively, induction of ATF4 by thiol oxidation is not dependent on common oxidative stress-induced pathways such as Nrf2, HRI, or HIF-1α.

ATF4 Is Important for CD4^{+} T Cell Activation and Proliferation

We first sought to determine whether ATF4 plays any significant role during T cell activation *in vitro*. As expected, the naive CD4^{+} T cells enlarged upon activation (Figure 2A), with T cells with β-ME being larger than those without β-ME. In contrast, the size of *Atf4*$^{-/-}$ CD4^{+} T cells was significantly smaller than WT CD4^{+} T cells, even in the presence of β-ME (Figure 2A). *Atf4*$^{-/-}$ CD4^{+} T cells completely failed to increase in size when cultured without β-ME, suggesting a possible defect in mass accumulation (Figure 2A).

T cell activation is followed by clonal expansion, which is controlled by cell survival and proliferation. ATF4 did not significantly affect T cell survival in both β-ME-sufficient and β-ME-deficient media (Figure 2B). In addition, ATF4 promoted DNA synthesis and T cell

division in β-ME-supplemented culture media (Figures 2C and 2D). ATF4 was critically important for proliferation when T cells were cultured in the absence of β-ME (Figures 2C and 2D). Similar to *Atf4*, deletion of *Gcn2* also resulted in decreases in proliferation (Figure S4). This result is consistent with a similar role of GCN2 in $CD8^+$ T cells (Van de Velde et al., 2016) and suggests overlapping function of GCN2 and ATF4 in activation-induced T cell proliferation. We also noted that $CD4^+$ T cells cultured in the Th1 condition seemed to be more dependent on ATF4 for proliferation compared with those in the Th17 condition (Figure 2D). Moreover, the analysis of gene profiling data indicated that ATF4 enhanced proliferation related genes (Table S2). Collectively, these data demonstrate that ATF4 promotes proliferation of activated $CD4^+$ T cells.

ATF4 Regulates Cysteine and GSH Metabolism in Response to the Extracellular Oxidizing Environment

Because cysteine is a key precursor for GSH, we performed two assays to measure intracellular GSH levels. First, we stained T cells with monochlorobimane (mBCI), which is nonfluorescent until conjugated with GSH, allowing quantification of GSH. We found that T cells cultured in the presence of β-ME had much greater amounts of GSH than those cultured in the absence of β-ME (Figure 3A). When buthionine sulfoximine (BSO), an inhibitor of gamma-glutamylcysteine synthetase (gamma-GCS), was added to the culture, the GSH levels were reduced, supporting the specificity of the assay (Figure 3A). Total GSH/GSSG was further quantified using an enzymatic recycling method (Rahman et al., 2006). Likewise, we found that addition of β-ME increased total GSH levels in T cells (Figure 3B).

The intracellular redox status is determined largely by GSH and its oxidized form, GSH disulfide (GSSG). Because of its high concentration inside cells, reduced glutathione, GSH, and its oxidized form, GSSG, constitute an important intracellular redox buffer system. We then examined the intracellular redox status using the 2′,7′-dichlorofluorescin diacetate (DCFDA) assay, a fluorogenic dye-based assay that measures hydroxyl, peroxyl, and other ROS activities (Halliwell and Whiteman, 2004). Indeed, T cells cultured without β-ME had greatly increased DCFDA signals compared with those cultured with β-ME (Figure 3C), suggesting that the extracellular oxidative environment can affect intracellular oxidative homeostasis through GSH. In addition, BSO led to an increase in oxidative stress in T cells as measured by DCFDA (Figure 3D), suggesting that GSH levels are important in maintaining redox homeostasis in T cells. Besides cysteine, glutamine is another key precursor for GSH synthesis. Lack of glutamine in the culture media induced oxidative stress in T cells (Figure S5A). Collectively, these data suggest that extracellular oxidizing environment and lack of glutamine strongly influence the intracellular redox status through controlling GSH levels.

Both NOX and mitochondrial sources of ROS are involved in regulating the redox status in T cells. We found that DCFDA signals were significantly reduced in *Ncf1*$^{-/-}$ T cells compared with WT control in the presence of β-ME (Figure 3E). However, in the absence of β-ME, the contribution of NCF1 to the intracellular ROS levels was minimal (Figure 3E). We also found that the XJB-5-113, a mitochondrially targeted ROS scavenger (Frantz et al.,

2013; Hoye et al., 2008), inhibited mitochondrial ROS as measured by MitoSox staining (Figure S5B) but did not inhibit intracellular oxidizing capacity in $CD4^+$ T cells regardless of β-ME presence (Figure 3F). Our data also indicated that a reduction in GSH levels when T cells were cultured without β-ME resulted in decreased mitochondrial ROS levels as measured by MitoSox staining (Figure S5C), suggesting that normal levels of GSH are required for mitochondrial functions. Collectively, these data suggest that in the extracellular oxidative environment, reduction of GSH levels, rather than ROS production by mitochondria and NOX, chiefly causes intracellular oxidative stress.

Next, we sought to determine whether ATF4 is involved in regulating GSH levels in activated T cells. Indeed, we found that the level of GSH was much lower in *Atf4*$^{-/-}$ $CD4^+$ T cells compared with WT control (Figure 3G). In addition, the level of total GSH was greatly reduced in ATF4-deficient T cells compared with WT T cells (Figure 3H). Because GSH levels were shown to be important for T cell proliferation (Suthanthiran et al., 1990), the decreased proliferation of *Atf4*$^{-/-}$ T cells can be due partly to decreases in GSH.

ATF4 Drives the T Cell Metabolic Reprogramming to Promote Amino Acid Synthesis

In order to understand the molecular mechanisms underpinning the function of ATF4 during early T cell activation, we performed gene expression profiling comparing WT and *Atf4*$^{-/-}$ $CD4^+$ T cells cultured without β-ME. An analysis of the top-ranked genes revealed that they are involved mainly in metabolism, bioenergetics, proliferation, and protein translation (Table S3).

Analysis of genes involved in amino acid metabolism (Table S4) suggested that ATF4 might drive expression of a co-ordinated cascade of genes that increase amino acid import, re-programed metabolic flux of amino acids through the TCA cycle, and promoted cysteine synthesis (Figure 4A). The first set of genes consists of amino acid transporters (Figure 4B; Tables S3 and S4). For example, expression of *Slc1a4* (also called ASCT1), a neutral amino acid transporter largely selective for alanine, serine, and cysteine but which can also be used to transport threonine and asparagine, was increased more than 10-fold in $CD4^+$ T cells stimulated in the absence of β-ME compared with those cultured in the presence of β-ME (Figure 4B). The expression of *Slc1a4* was greatly diminished in *Atf4*$^{-/-}$ $CD4^+$ T cells regardless of β-ME (Figure 4B). Similarly, *Slc7a3*, which encodes a transporter for arginine, lysine, and ornithine in a sodium-independent manner, was also upregulated by both ATF4 and the absence of β-ME (Tables S3 and S4). In addition, *Glyt1* was also greatly upregulated in WT upon cysteine restriction compared with *Atf4*$^{-/-}$ $CD4^+$ T cells (Figures S1A and S1B). Thus, on the basis of these data, the extracellular stress-induced ATF4 increases amino acid transporters, thereby increasing the import of amino acids including cysteine.

The analysis of genes regulated by ATF4 also revealed that cysteine synthesis is programmed to increase at multiple levels (Figure 4A). Serine has been recognized as an important precursor of cysteine because it interacts with homocysteine to form cystathione, which can be further broken down by 3-phosphoglycerate cystathionine gamma-lysase (Cth) to cysteine and α-ketobutyrate. *Cth* was greatly upregulated by ATF4 (Figure 4C; Table S3). In addition, the expression of two key enzymes involved in serine synthesis from 3-phosphoglycerate, 3-phosphoglycerate dehydrogenase (*Phgdh*) and phosphoserine

phosphatase (*Psph*), was also induced in an ATF4-dependent manner (Table S3). Thus, synthesis of cysteine and its precursor, serine, is upregulated by ATF4.

Further analysis revealed that additional genes are involved in channeling precursors for cysteine synthesis through the TCA cycle. Phosphoenolpyruvate carboxylase (*Pck2*) was highly up-regulated by ATF4 (Figure 4D; Table S3). PCK2 has an important cataplerotic function of catalyzing the generation of phosphoenopyruvate (PEP), a key precursor for serine synthesis, from TCA intermediate oxaloacetate (OAA) (Kalhan and Hanson, 2012; Stark and Kibbey, 2014). Therefore, ATF4 promotes anabolic processes by providing precursors for serine and eventually cysteine synthesis (Figure 4A).

Besides driving cataplerosis, ATF4 also upregulated enzymes that drive anaplerotic reactions replenishing the TCA cycle. Glutamic pyruvate transaminase (GPT2), which can catalyze the transfer of one amino group from glutamate to pyruvate, thus generating alanine and α-ketoglutarate, was upregulated by ATF4 (Figures 4A and 4E; Table S3). Thus, ATF4 might regulate amino acid metabolism through the TCA cycle.

Another main category of genes regulated by ATF4 were tRNA synthetases (Table S4). Cysteinyl-tRNA synthetase (Cars), the protein that promotes the charging of cysteine to its cognate tRNA, was upregulated in WT cells but not the *Atf4*$^{-/-}$ T cells (Figure 4F). These data suggest that ATF4 promotes protein translation, thereby allowing T cells to adapt to the reduction of amino acid levels.

mTORC1 is a central energy hub for sensing and regulating metabolism and availability of amino acid regulation of the mTOC1 activities (Chi, 2012). ATF4 deficiency resulted in a modest but significant decrease in mTORC1 activities, as assayed by the level of p-S6 by flow cytometry, in CD4^{+} T cells when cultured in the presence of β-ME (Figure 5A). Moreover, ATF4 is critical in maintaining the level of mTORC1 activities when CD4^{+} T cells were cultured without β-ME (Figure 5A). Besides p-S6, analysis of activation status of other mTORC1 pathway proteins such as p-mTOR, two forms of p-p70S6K, and p-4E-BP1 confirmed that ATF4 promoted mTORC1 activation in CD4^{+} T cells, particularly when cultured without β-ME (Figure 5B). This is likely because ATF4 is required for maintaining the protein (Figure 5B) but not mRNA level (Figure S6) of *Mtor*. Compared with *Atf4*, deletion of *Gcn2* resulted in relatively modest but significant decreases in mTORC1 activities as well (Figure 5B). Collectively, these data support an important role of ATF4 in metabolic reprograming, particularly during high extracellular thiol oxidation and amino acid restriction.

ATF4 Deficiency Resulted in Reduced Rates of Glycolysis and Oxygen Consumption in the Oxidative Environment during Early T Cell Activation

The gene expression profiling also suggested that glycolysis was regulated by ATF4 upon T cell activation (Figure 6; Table S4). Genes encoding the majority of enzymes in the glycolysis pathway were expressed at much higher levels in WT than in *Atf4*$^{-/-}$ CD4^{+} T cells (Figure 6A). We confirmed the expression of *Tpi1* gene by RT-qPCR (Figure 6B). To characterize the glycolysis in WT and *Atf4*$^{-/-}$ CD4^{+} T cells, we examined the extracellular acidification rate (ECAR), which correlates with glycolytic activity. We found that WT

$CD4^+$ T cells cultured without β-ME had lower ECARs than those cultured in the presence of β-ME. In contrast, *Atf4*$^{-/-}$ $CD4^+$ T cells had greatly reduced ECARs regardless of the culture condition (Figure 6C). Therefore, ATF4 is important in maintaining the level of glycolysis in activated $CD4^+$ T cells.

In aerobic organisms, all oxidative steps in the degradation of carbohydrates, fats, and amino acids culminate in oxidative phosphorylation, which drives the synthesis of ATP. Our gene expression profiling revealed that many genes that form complexesof the electronic transport chain have been downregulated in *Atf4*$^{-/-}$ $CD4^+$ T cells, suggesting that ATF4 is involved in promoting oxidative phosphorylation (Figures 6D and 6E; Table S4). We quantified oxygen consumption rate (OCR) as a measure of the level of mitochondrial respiration. We found that WT $CD4^+$ T cells cultured without β-ME had lower OCRs as well as ATP levels than those cultured in the presence of β-ME (Figures 6F and 6G). In addition, *Atf4*$^{-/-}$ $CD4^+$ T cells had significantly reduced OCRs and levels of ATP compared with WT $CD4^+$ T cells (Figures 6F and 6G). Therefore, ATF4 is important for maintaining the level of oxidative phosphorylation in activated $CD4^+$ T cells.

ATF4 Is Required for Th1 Immune Responses

We next sought to determine whether ATF4 is required for *in vitro* differentiation of T helper cell (Th) subsets. In the Th1 condition, addition of β-ME significantly increased T-bet levels, and ATF4 deficiency resulted in significantly reduced levels of T-bet in the presence of β-ME (Figure S7A). β-ME did not have great effect on RORgt expression. *Atf4* deletion resulted in modest but statistically significant reduction of RORgt in $CD4^+$ T cells cultured in the Th17 conditions. In the Th2 condition, addition of β-ME also significantly increased *Gata3* levels, but *Atf4* deficiency did not significantly affect the mRNA level of *Gata3* regardless of β-ME (Figure S7A). In the Treg culture, *Foxp3* levels were not affected by β-ME. *Atf4* deletion in T cells actually resulted in increased *Foxp3* mRNA levels when $CD4^+$ T cells were cultured without β-ME (Figure S7A). These results indicate that Th1 differentiation is preferentially dependent on ATF4 *in vitro*.

WT $CD4^+$ T cells cultured with β-ME in the Th1-polarizing conditions produced significantly higher amounts of IFN-γ upon re-stimulation (Figure 7A), whereas addition of β-ME only slightly increased IL-17 production for $CD4^+$ T cells cultured in Th17 conditions (Figure 7A). *Atf4* deficiency resulted in a greatly reduced IFN-γ production by $CD4^+$ T cells cultured in the Th1 condition regardless of β-ME (Figure 7A). When T cells were cultured in the Th17 condition, ATF4 deficiency did not lead to significant reduction in IL-17 in T cells cultured with β-ME and resulted in only a modest decrease of IL-17 in the absence of β-ME. Collectively, these data suggest that ATF4 is required for the IFN-γ production by Th1 cells, particularly when T cells are in the higher oxidizing environment.

The role of ATF4 in $CD4^+$ T cell-mediated autoimmune responses *in vivo* was then studied using the EAE model. WT or *Atf4*$^{-/-}$ 13.5 day fetal liver cells were infused into lethally irradiated B6 mice. Two months after infusion, we elicited EAE in these mice. Compared with mice transferred with WT fetal liver cells (WT FLT), mice infused with *Atf4*$^{-/-}$ fetal liver cells (*Atf4* knockout [KO] FLT) developed more severe signs of EAE (Figure 7B). Consistent with our *in vitro* data, MOG35–55-specific Th1 responses were reduced in

*Atf4*KO FLT mice compared with WT FLT mice (Figure 7C). Th17 cells are a causative factor in this model of EAE (Gonzalez-García et al., 2009; Langrish et al., 2005; Park et al., 2005). Consistent with the severity of EAE, we found that levels of MOG35–55-specific IL-17 were much higher in *Atf4*KO FLT mice than in WT FLT mice (Figure 7C). The reduced Th1 but increased Th17 immune responses were also observed when keyhole limpet hemocyanin (KLH) was used as the antigen (Figure S7B). These data indicated that ATF4 promoted Th1 but inhibited Th17 immune responses *in vivo*.

GCN2 deficiency led to decreases in both MOG-specific Th1 and Th17 immune responses (Figure S7C). However, GCN2 deficiency did not result in significant differences in the clinical signs of EAE (Figure S7D), suggesting a different *in vivo* role of ATF4 and GCN2 in this model of autoimmunity.

Because $Atf4^{-/-}$ $CD4^{+}$ T cells did not show increases of IL-17 production *in vitro*, we suspected that ATF4 deletion might affect the Th17-promoting cytokines in non-T cells. Because ATF4 deletion resulted in redox dysregulation and increased ROS levels were shown to induce elevated IL-1β production in myeloid cells (Allen et al., 2009), we decided to determine whether IL-1β levels in non-T cells were affected by ATF4 deletion. Indeed, we observed greater levels of IL-1β production in $Atf4^{-/-}$ APC *ex vivo* compared with WT APC (Figure 7D). We also found that Th17 cultures with $Atf4^{-/-}$ APC had greater frequencies of Th17 cells than those with WT APC (Figure 7E). In addition, blockade of IL-1β abrogated increases in IL-17 production (Figure 7E). These data suggest that ATF4 inhibits Th17 immune responses through non-T cells.

DISCUSSION

The oxidizing environment and availability of extracellular amino acids are major mechanisms that regulate T cell proliferation and function. Our data show that the extracellular oxidizing environment controls intracellular redox status through oxidation of molecules with thiol groups such as cysteine. The extracellular oxidizing environment induces ATF4 through GCN2-dependent as well as GCN2-independent mechanisms, whereas ATF4 induction as a result of the lack of glutamine and leucine is strictly dependent on GCN2. In addition, ATF4 is required for T cell redox homeostasis, proliferation, and cytokine production. Mechanistically, we demonstrate that ATF4 regulates amino acid metabolism, glycolysis, and oxygen consumption by driving a network of genes encoding proteins that control metabolic flux. ATF4 deficiency resulted in reduced Th1 and increased Th17 responses *in vivo*. These studies established an important role for ATF4 in T cell-mediated immune responses through metabolic reprogramming in responses to stress conditions.

The major effects of ATF4 induction include enhanced anabolic programs, resulting in importing amino acids, induction of *de novo* amino acid synthesis, and an increase of tRNA synthetases. The net consequence is an increase of amino acid and protein synthesis to ensure T cell proliferation in the stress environment (Krokowski et al., 2013). Another important purpose of this anabolic program is to maintain the level of GSH in T cells, necessary for intracellular redox homeostasis and proliferation. Although we have used

cysteine synthesis as an example to illustrate how ATF4 regulates amino acid anabolism, ATF4 certainly promotes synthesis of other non-essential amino acids. For example, an increase of serine can also lead to glycine synthesis. Likewise, the increase of ASNS can lead to increased ASN synthesis from ASP, which is generated from OAA by a cataplerotic reaction (Figure 4) (Zhang et al., 2014). Thus, ATF4 is important for maintaining levels of amino acids inside T cells by driving anabolic programs.

ATF4 also promotes catabolic metabolism such as glycolysis and glutaminolysis, thereby providing precursors for amino acid synthesis. First, ATF4 is important for glycolysis by upregulating many genes in the glycolysis pathway, leading to generation of pyruvate for the TCA cycle and providing carbon sources for amino acid synthesis and energy to fuel T cell growth. Second, ATF4 upregulated GPT2 (also called alanine transaminase [ALT]), which catalyzes conversion of L-glutamate and pyruvate to α-ketoglutarate and L-alanine, providing a key TCA substrate ketoglutarate and facilitating glutaminolysis. Thus, ATF4 promotes anaplerotic flux by enhancing glutaminolysis. Because several of the TCA cycle metabolites, such as citrate, OAA, and α-ketoglutarate, are respective precursors for the biosynthesis of amino acids, ATF4 increases amino acid anabolism through boosting anaplerotic reactions. Third, ATF4 increases *Pck2* gene, encoding a major cataplerotic enzyme in the synthesis of serine (Kalhan and Hanson, 2012). Thus, our analysis reveals a coordinated network of genes regulated by ATF4 leading to catabolism of major carbon and nitrogen sources of T cells, namely, glucose and glutamine, to satisfy the need of T cell growth, particularly in the oxidizing environment or when amino acids are limited. Future metabolic flux studies will be needed to further support our finding.

Finally, we showed that ATF4 deficiency resulted in reduced Th1 but increased Th17 responses *in vivo*, consistent with our *in vitro* data that Th1 cells are highly sensitive to ATF4 deficiency. T cell activation and proliferation, which is compromised by *Atf4* deficiency, are important for the development and effector functions of Th1 cells. The increased Th17 responses in $Atf4^{-/-}$ mice *in vivo* can be attributed to both a shift due to reduction of Th1 differentiation and elevated levels of Th17-driving factors in myeloid cells (Ravindran et al., 2016). Anjana Rao's group has shown that halofuginone suppresses Th17 responses by inducing amino acid starvation responses (Sundrud et al., 2009). Our data are consistent with their findings and further illustrate that ATF4 suppresses Th17 responses.

EXPERIMENTAL PROCEDURES

Mice

WT, $Gcn2^{-/-}$, $Nrf2^{-/-}$, and $Atf4^{+/-}$ mice were purchased from the Jackson Laboratory. HRI-deficient mouse spleen cells were from Dr. Jane-Jane Chen (MIT). *Ncf*-$1^{-/-}$ mice were from Dr. Jon Piganili (University of Pittsburgh). $Atf4^{-/-}$ on the Swiss Webster background were bred at the University of Pittsburgh. In order to generate fetal liver cell-reconstituted mice, $Atf4^{-/-}$ (on the C57BL6 background) or WT fetal liver cells, obtained from 13.5 day embryos, were injected intravenously (i.v.) into B6-LY5.2/Cr mice that had been irradiated at 9.5 Gy. Six- to 12-week-old mice were used. All experiments were conducted under an Institutional Animal Care and Use Committee-approved protocol and in accordance with NIH guidelines.

EAE Induction and *Ex Vivo* Analysis

Six- to 12-week-old mice were used for EAE induction by subcutaneous (s.c.) injection of 150 μg $MOG_{35–55}$(MEVGWYRSPFSRVVHLYRNGK) peptide in IFA plus 500 μg heat-inactivated *Mycobacterium tuberculosis*. Pertussis toxin (100 ng) was injected i.v. on days 0 and 2. Mice were monitored for clinical signs of EAE, scored as follows: 0 = normal; 1 = flaccid tail; 2 = hindlimb weakness or abnormal gait with poor ability to right from supine; 3 = partial hindlimb paralysis; 4 = both hindlimbs paralyzed with or without forelimb paralysis and incontinence; and 5 = moribund state. At day 22 of EAE induction, splenocytes were isolated from mice and cultured with 50 μg/mL $MOG_{35–55}$ for 72 hr.

KLH Induction and *Ex Vivo* Analysis

Eight-week-old female WT and $ATF4^{-/-}$ mice on the Swiss Webster background were immunized by footpad injection of 50 μg/mouse of KLH plus complete Freund's adjuvant (CFA). At day 8 after KLH injection, splenocytes and draining lymph nodes were isolated from mice and cultured with 50 μg/mL KLH for 72 hr.

Cell Culture

Naive $CD4^+$ T cells were cultured in 48-well plates precoated with 5 μg anti-CD3 (145-2C11) and 2.5 μg plate-bound anti-CD28 (37.51) monoclonal anti-bodies (mAbs) in RPMI 1640 with 10% fetal bovine serum (FBS). In some experiments, 50 μM β-ME or 2 mM NAC was added to the media. Th1, human IL-2 (20 U/mL), and murine IL-12 (3.4 ng/mL); Th0, human IL-2 (20 U/mL); Th17, murine IL-23 (10 ng/mL), murine IL-6 (10 ng/mL), TGF-β1 (1 ng/mL), anti-IFN-γ (10 μg/mL, clone XMG 1.2). PKR inhibitor (CAS 608512-97-6; Calbiochem), PERK inhibitor I (GSK2606414, CAS 1337531-89-1; Calbiochem), and the mitochondrially targeted ROS scavenger XJB-5-113 (from Dr. Peter Wipf, University of Pittsburgh) (Frantz et al., 2011; Rajagopalan et al., 2009) were added as indicated in experiments. Splenocyte-derived antigen-presenting cells were prepared by depleting T cells and natural killer (NK) cells with anti-Thy1 mAbs (Y19), anti-CD8 mAbs (53-6.72), anti-CD4 mAbs (GK1.5), and anti-NK1.1 mAbs (PK136) and rabbit complement in HANKS-10% FBS and subsequently irradiated at 3,000 rad.

Quantification of Signal Transduction by Western Blot and Flow Cytometry

The western blot antibodies include rabbit anti-ATF4 (Santa Cruz), mouse anti-TATA-box binding protein (Thermo Pierce), mTOR substrates antibody sampler kit (9862; Cell Signaling Technology). For flow cytometric analysis of pS6, anti-pS6 (Alexa Fluor 488; Cell Signaling Technology) was used.

BrdU Assay

T cells were stimulated and cultured for the indicated time, then washed and incubated with DPBS buffer with 1 mM BrdU (Thermo Fisher Scientific) at 37°C for 40 min. Cells were fixed by fixation buffer at room temperature for 30 min and then washed by permeabilization buffer (transcription factor fixation/permeabilization concentrate and diluent; eBioscience). Then cells were incubated with 100 μL DPBS with 300 μg/mL DNase (Sigma-Aldrich) at 37°C for 1 hr. Then cells were washed by 1 mL 13 BD Perm/Wash

Buffer, and the incubation with DNase solution was repeated. Cells were washed by permeabilization buffer and incubated with anti-BrdU-fluorescein isothiocyanate (FITC) (Invitrogen) at room temperature for 20 min and analyzed by flow cytometry.

Annexin V Assay

T cells were stimulated and cultured for the indicated time, then washed and incubated with 100 μL annexin V binding buffer with FITC annexin V (BioLegend) and 7-AAD (BioLegend) in the dark at room temperature for 15 min. Then 400 μL annexin V binding buffer was added to each sample. Cells were analyzed by flow cytometry.

Extracellular Flux and ATP Analysis

OCRs and ECARs were measured in XF media under basal condition on XF-24 Extracelluler Flux Analyzers according to the instructions of the manufacturer (Seahorse Bioscience). ATP measurement was done using the ATP Lite kit according to the instructions of the manufacturer (PerkinElmer).

GSH and ROS Assay

BSO (50 μM; Cayman) was added to the indicated samples at the onset of the culture. At 24 hr, cells were stained by 10 μM mBCI (Invitrogen) at 37°C for 15 min and analyzed by flow cytometry. For ROS level measurement, cells were stained by 2 μM H2-DCFDA at 37°C for 20 min and then recovered in c-RPMI at 37°C for another 20 min and then analyzed by flow cytometry. Total GSH measurement was performed according to previous description (Rahman et al., 2006).

MitoSox Assay

T cells were stimulated and cultured for indicated time, then washed and resuspended by 100 μL pre-warmed Hank's balanced salt solution (HBSS) buffer with 5 μM MitoSox (Thermo Fisher Scientific) and incubated at 37°C for 30 min. The MitoSox level of cells were then analyzed by flow cytometry.

Real-Time PCR Primers

The following primers were used for real-time PCR: b-*Actin*, 5′-GAAATCGTGCGTGACATCAAA-3′and 5′-TGTAGTTTCATGGATGCCACCG-3′; *Asns*, 5′-CACAAGGCGCTACAGCAAC-3′and 5′-CCAGCATACAGATGGTTTTCT CG-3′; A*tf*4, 5′-CCTGAACAGCGAAGTGTTGG-3′and 5′-TGGAGAACCCATGAGGTTTCAA-3′; *Slc1a4*, 5′-GGCATCGCTGTTGCTTACTTC-3′and 5′-CGA GGAAAGAGTCCACTGTCT-3′; *Slc1a5*, 5′-CATCAACGACTCTGTTGTAGACC-3′and 5′-CGCTGGATACAGGATTGCGG-3′; *Slc7a11*, 5′-AGGGCATACTCCAGAACACG-3′and 5′-GGACCAAAGACCTCCAGAATG-3′; *Cth*, 5′-GGCTTCCTGCCTAGTTTCCAG-3′and 5′-AGTCCTGCTTAAATGTGGTGG-3′; *Cars*, 5′-CATTCTGAGCATTAGTGACGAGG-3′and 5′-CTGCCTGAACACGTCCACAT-3′; *Gpt2*, 5′-AACCATTCACTGAGGTAATCCGA-3′and 5′-GGGCTGTTTAGTAGGTTTGGGTA-3′; *Tpi1*, 5′-

CCAGGAAGTTCTTCGTTGGGG-3′and 5′-CAAAGTCGATGTAAGCGGTGG-3′; *Ndufa3*, 5′-ATGGCCGGGAGAATCTCTG-3′and 5′-AGGGGCTAATCATGGGCATAAT-3′; *Pck2*, 5′-ATGGCTGCTATGTACCTCCC-3′and 5′-GCGCCACAAAGTCTCGAAC-3′.

Statistics

The unpaired two-tailed Student's t test was used for statistical analysis comparing two sets of data. ANOVA was used for comparison among more than two sets of data. Results were considered statistically significant at $p < 0.05$.

Supplementary Material

Refer to Web version on PubMed Central for supplementary material.

Acknowledgments

This project was supported mainly by the NIH through grants 1R21AI124676 (to B.L.), UL1 RR024153 (to B.L.), UL1TR000005 (to B.L.), and 1P50 CA097190 (to B.L.); Roswell Park Cancer Institute/University of Pittsburgh Cancer Institute Ovarian Cancer Specialized Programs of Research Excellence grant P50CA159981 (to B.L.); National Natural Science Foundation of China (NSFC) grants 31428005 (to B.L. and J.J.); NSFC grant 31320103918 (to X.Z. and B.L.); and NSFC grant 81273208 (to Y.Z.). X.Y. was supported by a scholarship from the NSFC. P.W. is supported by NIH/National Institute of Allergy and Infectious Diseases (NIAID) grant 1U19A168021. G.X. is supported by NSFC grant 81472049.

References

Allen IC, Scull MA, Moore CB, Holl EK, McElvania-TeKippe E, Taxman DJ, Guthrie EH, Pickles RJ, Ting JP. The NLRP3 inflammasome mediates in vivo innate immunity to influenza A virus through recognition of viral RNA. Immunity. 2009; 30:556–565. [PubMed: 19362020]

Ameri K, Harris AL. Activating transcription factor 4. Int J Biochem Cell Biol. 2008; 40:14–21. [PubMed: 17466566]

Angelini G, Gardella S, Ardy M, Ciriolo MR, Filomeni G, Di Trapani G, Clarke F, Sitia R, Rubartelli A. Antigen-presenting dendritic cells provide the reducing extracellular microenvironment required for T lymphocyte activation. Proc Natl Acad Sci USA. 2002; 99:1491–1496. [PubMed: 11792859]

Brindle PK, Montminy MR. The CREB family of transcription activators. Curr Opin Genet Dev. 1992; 2:199–204. [PubMed: 1386267]

Bronte V, Serafini P, Mazzoni A, Segal DM, Zanovello P. L-arginine metabolism in myeloid cells controls T-lymphocyte functions. Trends Immunol. 2003; 24:302–306. [PubMed: 12810105]

Chi H. Regulation and function of mTOR signalling in T cell fate decisions. Nat Rev Immunol. 2012; 12:325–338. [PubMed: 22517423]

Dong J, Qiu H, Garcia-Barrio M, Anderson J, Hinnebusch AG. Uncharged tRNA activates GCN2 by displacing the protein kinase moiety from a bipartite tRNA-binding domain. Mol Cell. 2000; 6:269–279. [PubMed: 10983975]

Dringen R, Gutterer JM, Hirrlinger J. Glutathione metabolism in brain metabolic interaction between astrocytes and neurons in the defense against reactive oxygen species. Eur J Biochem. 2000; 267:4912–4916. [PubMed: 10931173]

Frantz MC, Pierce JG, Pierce JM, Kangying L, Qingwei W, Johnson M, Wipf P. Large-scale asymmetric synthesis of the bioprotective agent JP4-039 and analogs. Org Lett. 2011; 13:2318–2321. [PubMed: 21452836]

Frantz MC, Skoda EM, Sacher JR, Epperly MW, Goff JP, Greenberger JS, Wipf P. Synthesis of analogs of the radiation mitigator JP4-039 and visualization of BODIPY derivatives in mitochondria. Org Biomol Chem. 2013; 11:4147–4153. [PubMed: 23715589]

Gjymishka A, Su N, Kilberg MS. Transcriptional induction of the human asparagine synthetase gene during the unfolded protein response does not require the ATF6 and IRE1/XBP1 arms of the pathway. Biochem J. 2009; 417:695–703. [PubMed: 18840095]

Gonzalez-García I, Zhao Y, Ju S, Gu Q, Liu L, Kolls JK, Lu B. IL-17 signaling-independent central nervous system autoimmunity is negatively regulated by TGF-beta. J Immunol. 2009; 182:2665–2671. [PubMed: 19234160]

Hai TW, Liu F, Coukos WJ, Green MR. Transcription factor ATF cDNA clones: an extensive family of leucine zipper proteins able to selectively form DNA-binding heterodimers. Genes Dev. 1989; 3(12B):2083–2090. [PubMed: 2516827]

Halliwell B, Whiteman M. Measuring reactive species and oxidative damage in vivo and in cell culture: how should you do it and what do the results mean? Br J Pharmacol. 2004; 142:231–255. [PubMed: 15155533]

Harding HP, Zhang Y, Zeng H, Novoa I, Lu PD, Calfon M, Sadri N, Yun C, Popko B, Paules R, et al. An integrated stress response regulates amino acid metabolism and resistance to oxidative stress. Mol Cell. 2003; 11:619–633. [PubMed: 12667446]

Hoye AT, Davoren JE, Wipf P, Fink MP, Kagan VE. Targeting mitochondria. Acc Chem Res. 2008; 41:87–97. [PubMed: 18193822]

Ishii T, Sugita Y, Bannai S. Regulation of glutathione levels in mouse spleen lymphocytes by transport of cysteine. J Cell Physiol. 1987; 133:330–336. [PubMed: 3680392]

Kalhan SC, Hanson RW. Resurgence of serine: an often neglected but indispensable amino Acid. J Biol Chem. 2012; 287:19786–19791. [PubMed: 22566694]

Karpinski BA, Morle GD, Huggenvik J, Uhler MD, Leiden JM. Molecular cloning of human CREB-2: an ATF/CREB transcription factor that can negatively regulate transcription from the cAMP response element. Proc Natl Acad Sci USA. 1992; 89:4820–4824. [PubMed: 1534408]

Kesarwani P, Al-Khami AA, Scurti G, Thyagarajan K, Kaur N, Husain S, Fang Q, Naga OS, Simms P, Beeson G, et al. Promoting thiol expression increases the durability of antitumor T-cell functions. Cancer Res. 2014; 74:6036–6047. [PubMed: 25164014]

Krokowski D, Han J, Saikia M, Majumder M, Yuan CL, Guan BJ, Bevilacqua E, Bussolati O, Bröer S, Arvan P, et al. A self-defeating anabolic program leads to β-cell apoptosis in endoplasmic reticulum stress-induced diabetes via regulation of amino acid flux. J Biol Chem. 2013; 288:17202–17213. [PubMed: 23645676]

Langrish CL, Chen Y, Blumenschein WM, Mattson J, Basham B, Sedgwick JD, McClanahan T, Kastelein RA, Cua DJ. IL-23 drives a pathogenic T cell population that induces autoimmune inflammation. J Exp Med. 2005; 201:233–240. [PubMed: 15657292]

Maciolek JA, Pasternak JA, Wilson HL. Metabolism of activated T lymphocytes. Curr Opin Immunol. 2014; 27:60–74. [PubMed: 24556090]

Munn DH, Mellor AL. Indoleamine 2,3 dioxygenase and metabolic control of immune responses. Trends Immunol. 2013; 34:137–143. [PubMed: 23103127]

Munn DH, Sharma MD, Baban B, Harding HP, Zhang Y, Ron D, Mellor AL. GCN2 kinase in T cells mediates proliferative arrest and anergy induction in response to indoleamine 2,3-dioxygenase. Immunity. 2005; 22:633–642. [PubMed: 15894280]

Park H, Li Z, Yang XO, Chang SH, Nurieva R, Wang YH, Wang Y, Hood L, Zhu Z, Tian Q, Dong C. A distinct lineage of CD4 T cells regulates tissue inflammation by producing interleukin 17. Nat Immunol. 2005; 6:1133–1141. [PubMed: 16200068]

Pedersen-Lane JH, Zurier RB, Lawrence DA. Analysis of the thiol status of peripheral blood leukocytes in rheumatoid arthritis patients. J Leukoc Biol. 2007; 81:934–941. [PubMed: 17210617]

Qiu H, Dong J, Hu C, Francklyn CS, Hinnebusch AG. The tRNA-binding moiety in GCN2 contains a dimerization domain that interacts with the kinase domain and is required for tRNA binding and kinase activation. EMBO J. 2001; 20:1425–1438. [PubMed: 11250908]

Rahman I, Kode A, Biswas SK. Assay for quantitative determination of glutathione and glutathione disulfide levels using enzymatic recycling method. Nat Protoc. 2006; 1:3159–3165. [PubMed: 17406579]

Rajagopalan MS, Gupta K, Epperly MW, Franicola D, Zhang X, Wang H, Zhao H, Tyurin VA, Pierce JG, Kagan VE, et al. The mitochondria-targeted nitroxide JP4-039 augments potentially lethal irradiation damage repair. In Vivo. 2009; 23:717–726. [PubMed: 19779106]

Ravindran R, Loebbermann J, Nakaya HI, Khan N, Ma H, Gama L, Ma-chiah DK, Lawson B, Hakimpour P, Wang YC, et al. The amino acid sensor GCN2 controls gut inflammation by inhibiting inflammasome activation. Nature. 2016; 531:523–527. [PubMed: 26982722]

Sahaf B, Heydari K, Herzenberg LA, Herzenberg LA. Lymphocyte surface thiol levels. Proc Natl Acad Sci USA. 2003; 100:4001–4005. [PubMed: 12642656]

Sena LA, Li S, Jairaman A, Prakriya M, Ezponda T, Hildeman DA, Wang CR, Schumacker PT, Licht JD, Perlman H, et al. Mitochondria are required for antigen-specific T cell activation through reactive oxygen species signaling. Immunity. 2013; 38:225–236. [PubMed: 23415911]

Shi LZ, Wang R, Huang G, Vogel P, Neale G, Green DR, Chi H. HIF1alpha-dependent glycolytic pathway orchestrates a metabolic checkpoint for the differentiation of TH17 and Treg cells. J Exp Med. 2011; 208:1367–1376. [PubMed: 21708926]

Srivastava MK, Sinha P, Clements VK, Rodriguez P, Ostrand-Rosenberg S. Myeloid-derived suppressor cells inhibit T-cell activation by depleting cystine and cysteine. Cancer Res. 2010; 70:68–77. [PubMed: 20028852]

Stark R, Kibbey RG. The mitochondrial isoform of phosphoenolpyruvate carboxykinase (PEPCK-M) and glucose homeostasis: has it been overlooked? Biochim Biophys Acta. 2014; 1840:1313–1330. [PubMed: 24177027]

Sundrud MS, Koralov SB, Feuerer M, Calado DP, Kozhaya AE, Rhule-Smith A, Lefebvre RE, Unutmaz D, Mazitschek R, Waldner H, et al. Halofuginone inhibits TH17 cell differentiation by activating the amino acid starvation response. Science. 2009; 324:1334–1338. [PubMed: 19498172]

Suthanthiran M, Anderson ME, Sharma VK, Meister A. Glutathione regulates activation-dependent DNA synthesis in highly purified normal human T lymphocytes stimulated via the CD2 and CD3 antigens. Proc Natl Acad Sci USA. 1990; 87:3343–3347. [PubMed: 1970635]

Tse HM, Thayer TC, Steele C, Cuda CM, Morel L, Piganelli JD, Mathews CE. NADPH oxidase deficiency regulates Th lineage commitment and modulates autoimmunity. J Immunol. 2010; 185:5247–5258. [PubMed: 20881184]

Van de Velde LA, Guo XJ, Barbaric L, Smith AM, Oguin TH 3rd, Thomas PG, Murray PJ. Stress kinase GCN2 controls the proliferative fitness and trafficking of cytotoxic T cells independent of environ-mental amino acid sensing. Cell Rep. 2016; 17:2247–2258. [PubMed: 27880901]

Vazquez de Aldana CR, Wek RC, Segundo PS, Truesdell AG, Hinnebusch AG. Multicopy tRNA genes functionally suppress mutations in yeast eIF-2 alpha kinase GCN2: evidence for separate pathways coupling GCN4 expression to unchanged tRNA. Mol Cell Biol. 1994; 14:7920–7932. [PubMed: 7969132]

Wek RC, Jackson BM, Hinnebusch AG. Juxtaposition of domains homologous to protein kinases and histidyl-tRNA synthetases in GCN2 protein suggests a mechanism for coupling GCN4 expression to amino acid availability. Proc Natl Acad Sci USA. 1989; 86:4579–4583. [PubMed: 2660141]

Wek SA, Zhu S, Wek RC. The histidyl-tRNA synthetase-related sequence in the eIF-2 alpha protein kinase GCN2 interacts with tRNA and is required for activation in response to starvation for different amino acids. Mol Cell Biol. 1995; 15:4497–4506. [PubMed: 7623840]

Zhang Y, Xiang Y. Molecular and cellular basis for the unique functioning of Nrf1, an indispensable transcription factor for maintaining cell homoeostasis and organ integrity. Biochem J. 2016; 473:961–1000. [PubMed: 27060105]

Zhang J, Fan J, Venneti S, Cross JR, Takagi T, Bhinder B, Djaballah H, Kanai M, Cheng EH, Judkins AR, et al. Asparagine plays a critical role in regulating cellular adaptation to glutamine depletion. Mol Cell. 2014; 56:205–218. [PubMed: 25242145]

Zhu S, Sobolev AY, Wek RC. Histidyl-tRNA synthetase-related sequences in GCN2 protein kinase regulate in vitro phosphorylation of eIF-2. J Biol Chem. 1996; 271:24989–24994. [PubMed: 8798780]

Highlights

- Oxidizing environments and amino acid starvation induce ATF4 in $CD4^+$ T cells
- ATF4 increases mTORC1 activation plus intake and *de novo* synthesis of amino acids
- ATF4 enhances glycolysis, glutaminolysis, and oxidative phosphorylation
- ATF4 deficiency leads to decreases in Th1 but increases in Th17 immune responses.

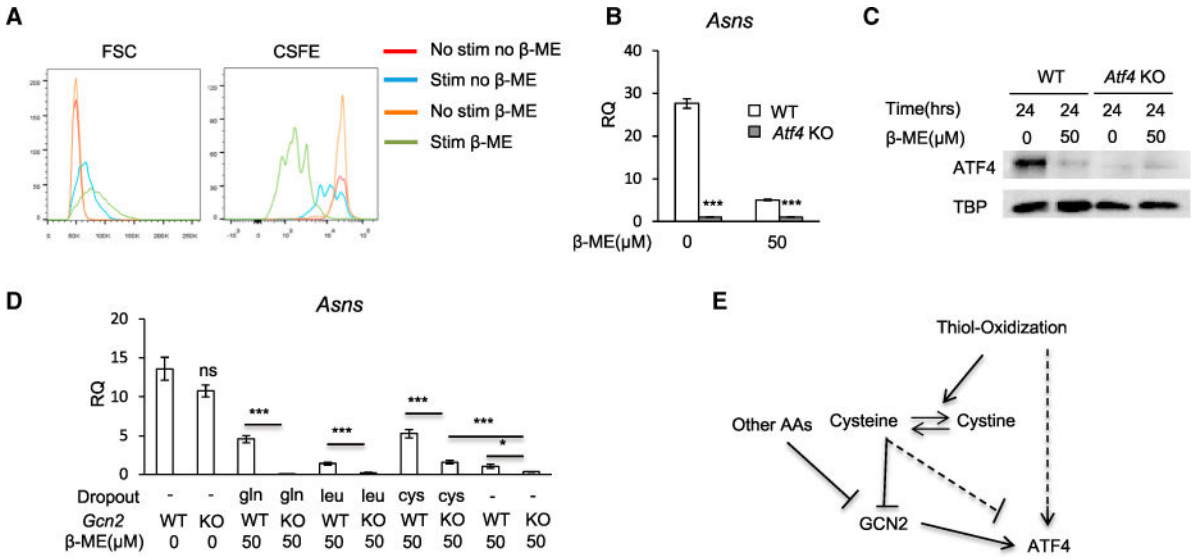

Figure 1. The Oxidative Environment and Amino Acid Deprivation Induced ATF4 Expression in T Cells

(A) Primary $CD4^+$ T cells were labeled with carboxyfluorescein succinimidyl ester (CFSE) and stimulated under the Th1 polarizing condition. Cell size (left) and proliferation (right) were detected by flow cytometry at 24 and 72 hr, respectively.

(B) WT and *Atf4* KO $CD4^+$ T cells were stimulated under Th1 condition. At 24 hr, mRNA level of ATF4 downstream gene *Asns* were analyzed by RT-qPCR.

(C) WT and *Atf4* KO $CD4^+$ T cells were stimulated under a Th1 condition. At 24 hr, nuclear extracts were made and analyzed by western blot.

(D) WT and *Gcn2* KO $CD4^+$ T cells were stimulated under a Th1 condition for 24 hr. Different amino acids were dropped out from the media. mRNA level of ASNS was analyzed by RT-qPCR.

(E) Schematic diagram of the regulatory effect of amino acid availability and oxidizing environment on ATF4.

*p < 0.05 and ***p < 0.005. Data are mean ± SEM. Student's t test was performed. See also Figures S1–S3 and Table S1.

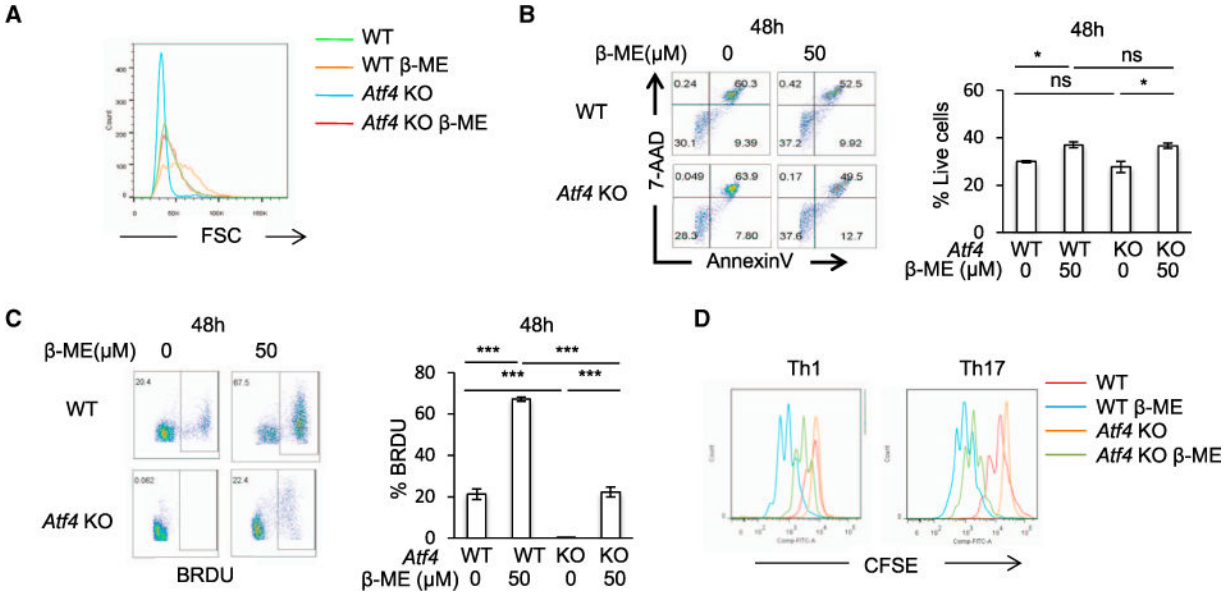

Figure 2. *Atf4*-Deficient Th1 Cells Have Impaired Cell Blasting, Proliferation, and Effector Functions

(A) Primary WT and *Atf4* KO CD4$^+$ T cells were stimulated in the presence or absence of β-ME for 24 hr. (B and C) Primary CD4$^+$ T cells were stimulated in a Th1 polarizing condition for 48 h. Proliferation and cell death were detected by BRDU (B) or annexin V/ 7AAD (C).

(D) Primary CD4$^+$ T cells were stained by CFSE and stimulated in the presence or absence of β-ME under a Th1 or a Th17 polarizing culture condition for 72 h.

*$p < 0.05$ and ***$p < 0.005$. Data are mean ± SEM. One-way ANOVA was performed. See also Figure S4 and Table S2.

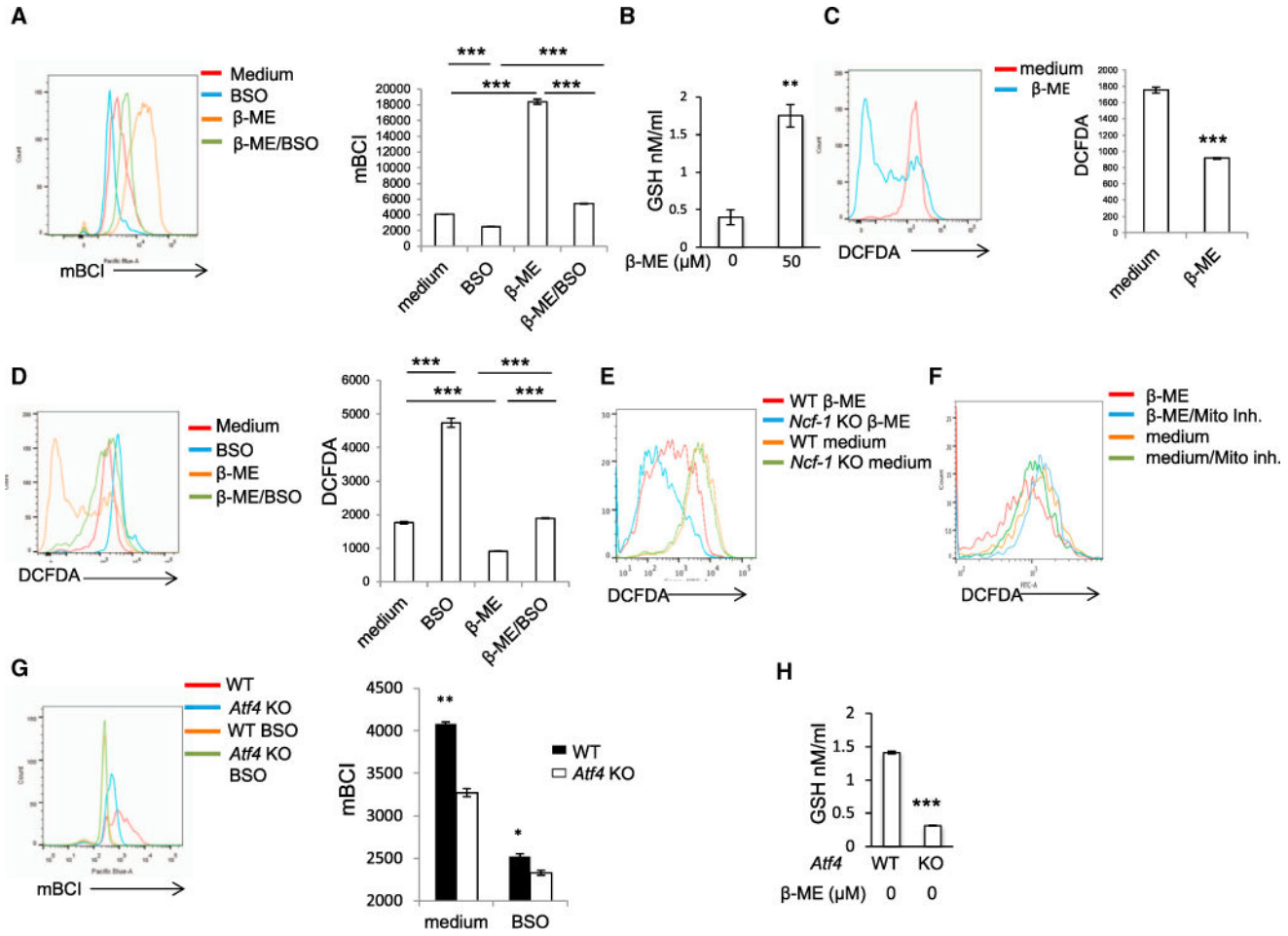

Figure 3. ATF4 Regulates GSH Level in CD4$^+$ T Cells

(A–D) CD4$^+$ T cells were stimulated in the presence or absence of BSO or β-ME. At 24 hr, total GSH was stained by mBCI (A) or enzymatic recycling method (B), and intracellular ROS were measured by DCFDA (C and D).

(E) WT and *Ncf-1* KO CD4$^+$ T cells were stimulated in the presence or absence of β-ME. At 24 hr, intracellular ROS were stained by DCFDA.

(F) CD4$^+$ T cells were stimulated in the presence or absence of β-ME or mitochondrial ROS scavenger XJB-5-113. At 24 hr, intracellular redox status was determined by the DCFDA staining assay.

(G and H) WT and *Atf4* KO CD4$^+$ T cells were stimulated in the presence or absence of BSO. At 24 hr, GSH levels were determined by mBCI staining (G) or the enzymatic recycling method (H).

*p < 0.05, **p < 0.01, and ***p < 0.005. Data are mean ± SEM. One-way ANOVA and Student's t test were performed. See also Figure S5.

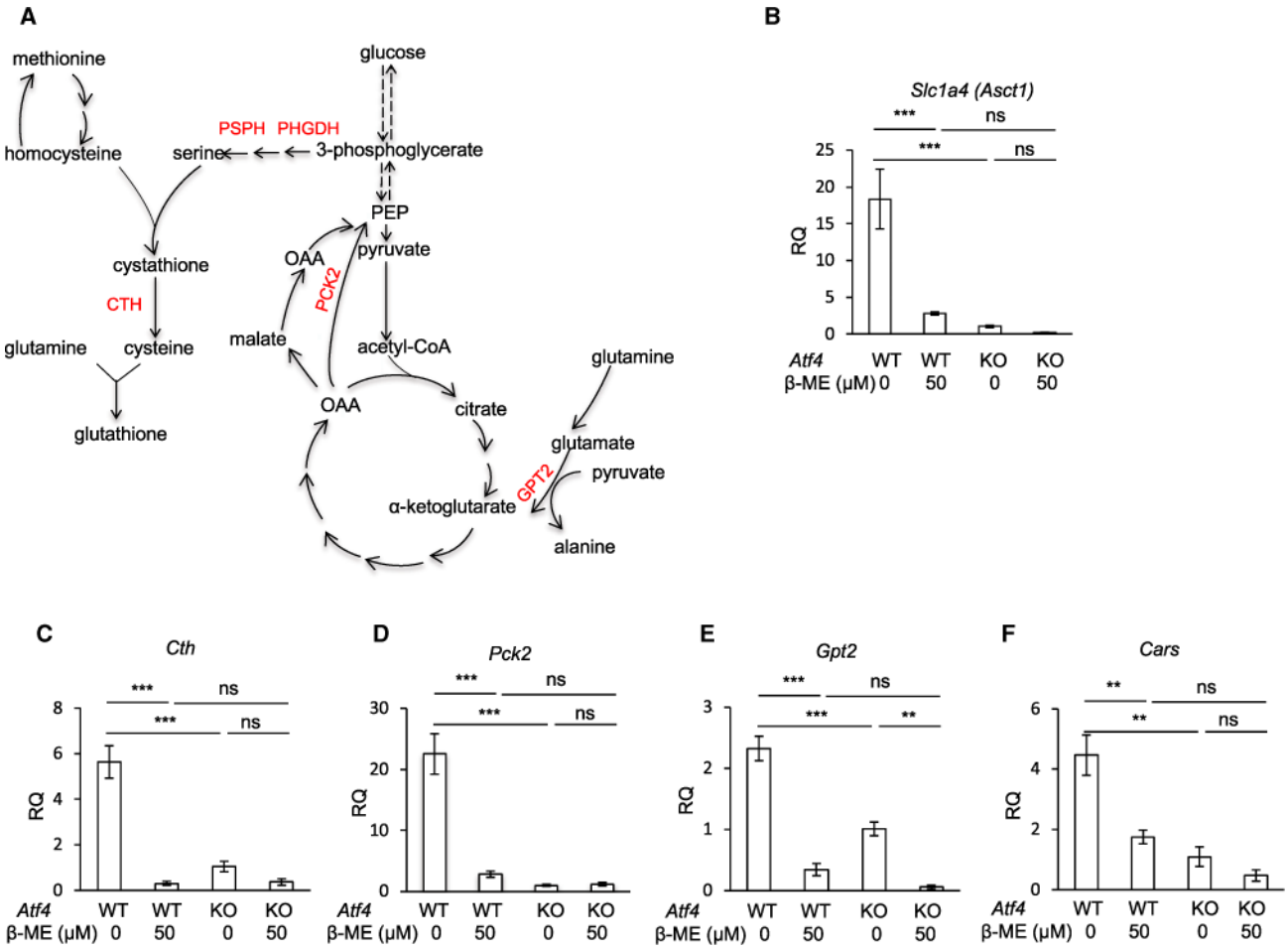

Figure 4. ATF4 Regulates Genes Involved in Cysteine Uptake and Synthesis

(A) Schematic drawing of glutaminolysis, the TCA cycle, and the cysteine synthesis pathway. The genes upregulated in ATF4-intact cells are highlighted in red.

(B–F) WT and *Atf4* KO $CD4^+$ T cells were stimulated in the presence or absence of β-ME for 24 hr. Cysteine transporter (B), cysteinyl-tRNA synthetase (C), cystathionase (D), glutamate pyruvate transaminase 2 (E) and phosphoenolpyruvate carboxykinase 2 (F) were analyzed by RT-qPCR.

**p < 0.01 and ***p < 0.005. Data are mean ± SEM. One-way ANOVA and Student's t test were performed. See also Tables S3 and S4.

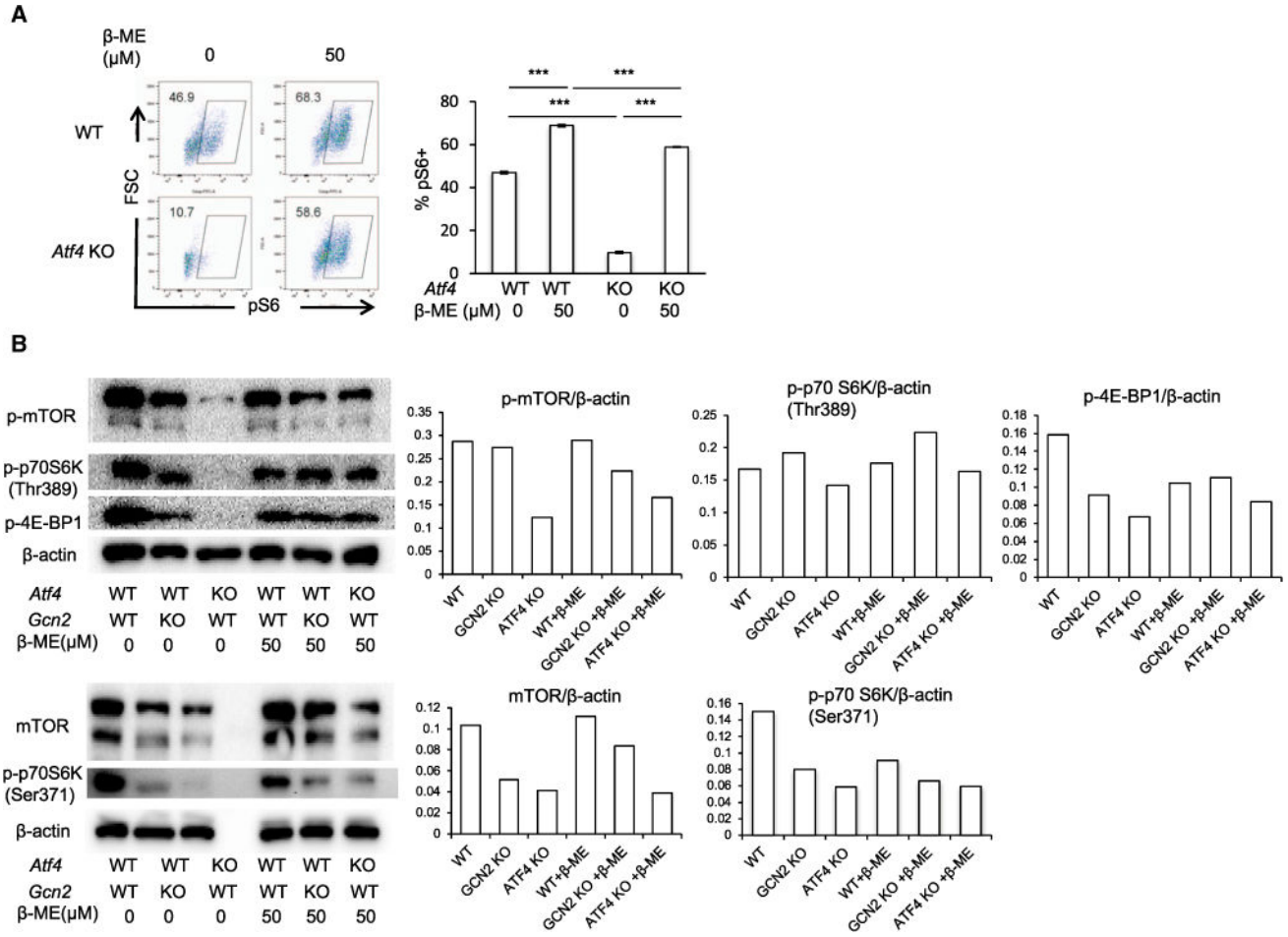

Figure 5. ATF4 Regulates mTORC1 Pathway

Primary WT and *Atf4* KO CD4$^+$ T cells were stimulated under Th1 polarizing condition for 72 hr.

(A) Cells were counted and re-stimulated by plate-bound anti-CD3 for 6 hr. p-S6 was detected by flow cytometry.

(B) Important proteins involved in mTORC1 pathway were analyzed by western blot (left). The quantification of western blot bands is shown in bar charts (right).

***p < 0.005. Data are mean ± SEM. One-way ANOVA and Student's t test were performed. See also Figure S6.

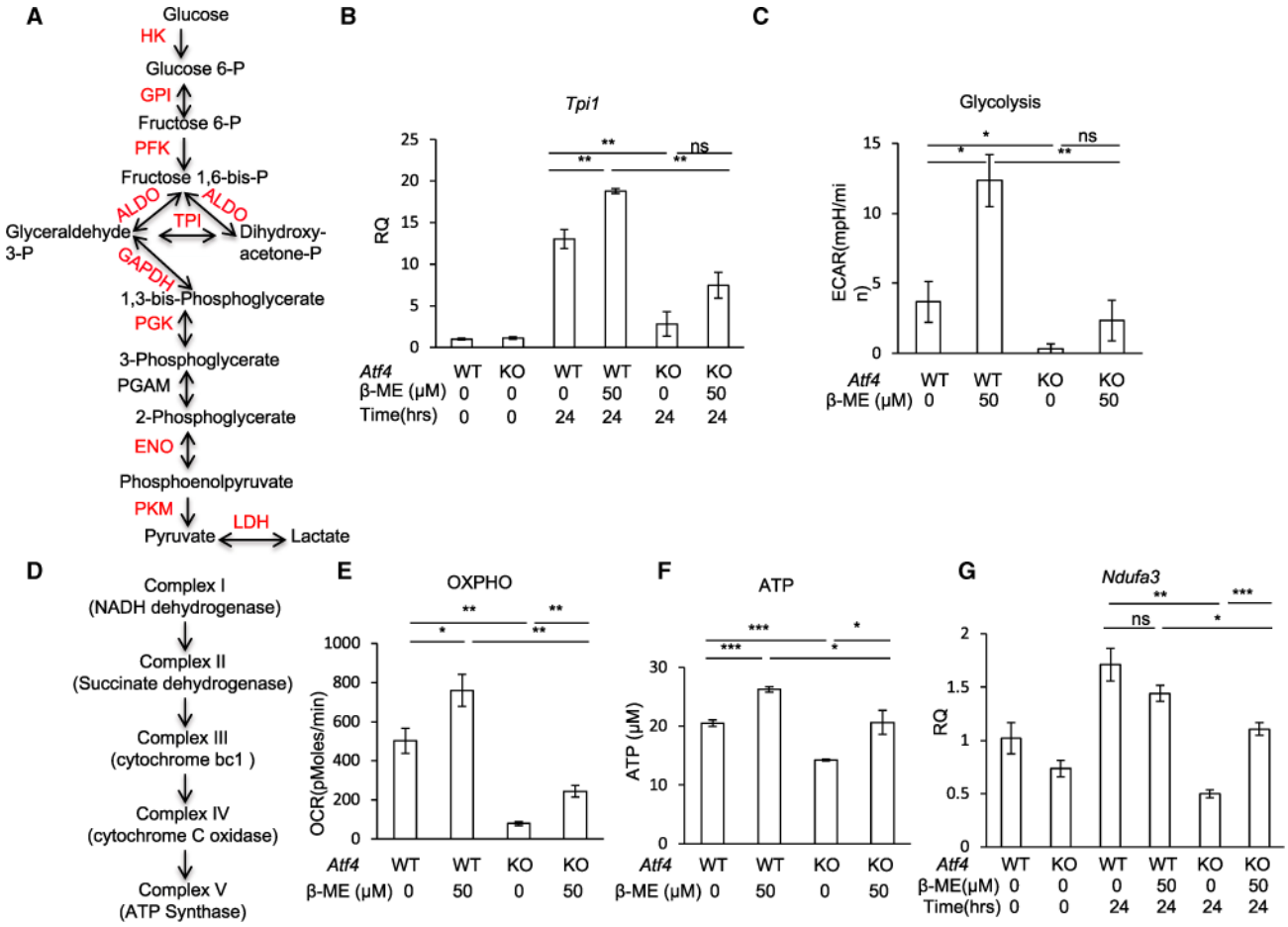

Figure 6. *Atf4* KO CD4$^+$ T Cells Are Impaired in Glycolysis and Oxidative Respiration

(A) Schematic drawing of the glycolysis pathway. Genes upregulated by ATF4 were highlighted in red.

(B and C) Primary WT and *Atf4*KO CD4$^+$ T cells were stimulated in the presence or absence of β-ME for 24 hr. The expression of Tip1 (B) was quantified by RT-qPCR. Glycolysis (C) was analyzed by XF24 Seahorse machine.

(D) The schematic drawing of the complexes of the respiratory chain.

(E–G) CD4$^+$ T cells were stimulated in the presence or absence of β-ME for 24 hr. The expression of *Ndufa3* (E) was quantified by RT-qPCR. OXPHOS (F) was analyzed by XF24 Seahorse machine. ATP levels in these cells (G) were measured by ATPlite kit.

*p < 0.05, **p < 0.01, and ***p < 0.005. Data are mean ± SEM. One-way ANOVA was performed.

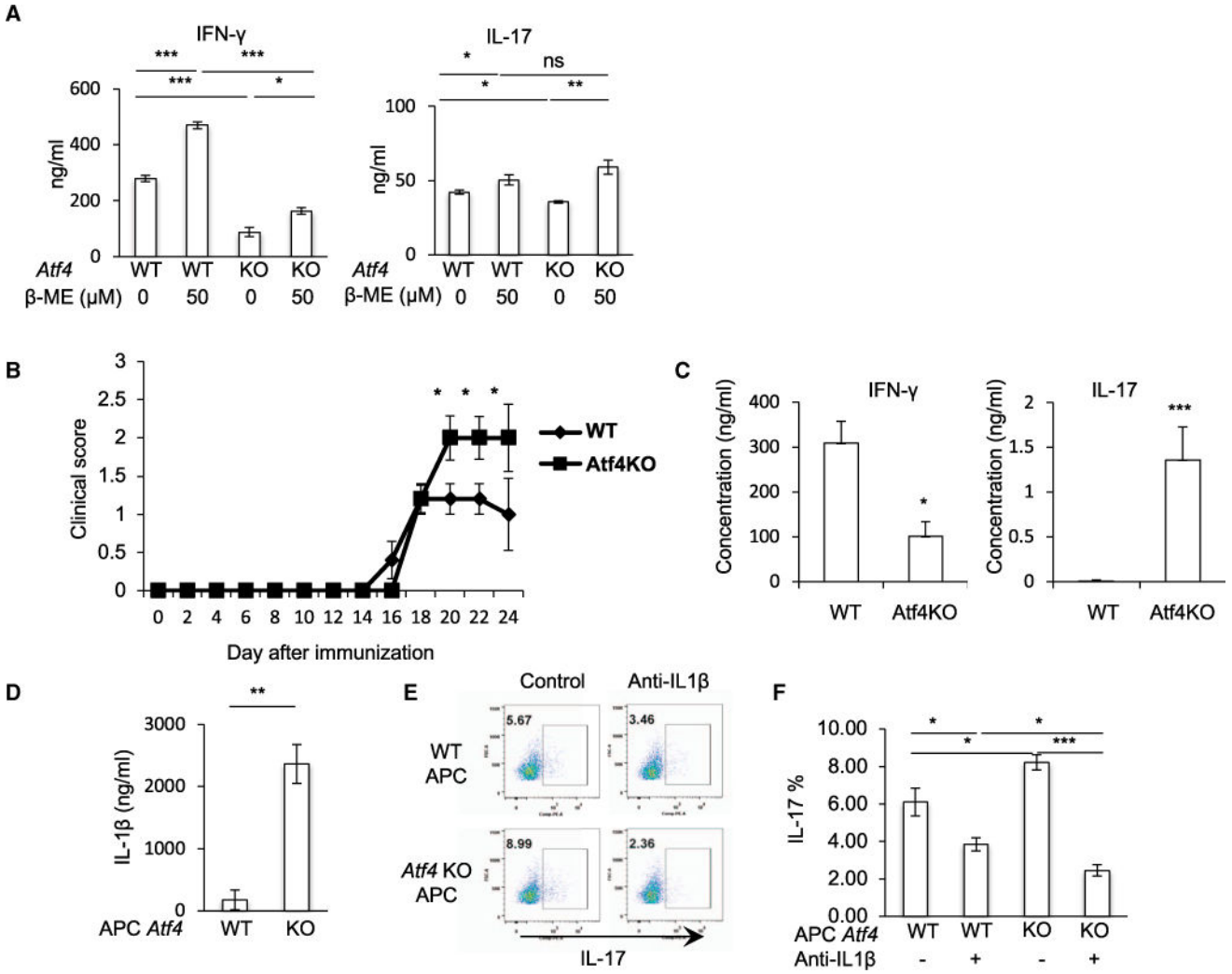

Figure 7. ATF4 Regulates Th1 and Th17 Immune Responses *In Vitro* and *In Vivo*

(A) WT and *Atf*4 KO CD4$^+$ T cells were stimulated in the presence or absence of β-ME under Th1 and Th17 polarizing conditions. At 96 hr, cells were re-stimulated by plate-bound anti-CD3 for 16 hr.

(B) WT FLT and *Atf4* KO FLT (both donor and recipient mice on the C57BL/6 background) were immunized with MOG35–55 peptides in CFA and pertussis toxin. Clinical scores were recorded every 2 days. Data were representative of three independent experiments.

(C) Mice were sacrificed at day 22, and splenocytes were isolated and stimulated with 50 μg MOG35–55 peptides *ex vivo* for 3 days. All cells were cultured in the presence of β-ME. At 72 hr, supernatants were collected and then analyzed by ELISA.

(D) Co-cultures were set up with antigen-presenting cells (APCs) isolated from splenocytes of WT and *Atf4*KO mice that had been immunized with MOG35–55 peptides and CFA for 10 days and CD4$^+$ T cells from unimmunized mice under the Th17 polarizing condition.

(E) Some supernatants were collected at 48 hr, and IL-1β levels were analyzed by ELISA. At 72 hr, cells were counted and restimulated by PMA/ionomycin for 4 hr.

(F) Frequencies of IL-17 producers were then analyzed by flow cytometry.

*p < 0.05, **p < 0.01, and ***p < 0.005. Data are mean ± SEM. Student's t test was performed. See also Figure S7.